AWARD NUMBER: **W81XWH-16-1-0533**

TITLE: Targeting the CRMP2-Ca2+ Channel Complex for Abortive Treatment of Migraine and Posttraumatic Headache

PRINCIPAL INVESTIGATOR: Rajesh Khanna, Ph.D.

CONTRACTING ORGANIZATION: University of Arizona
Tucson, AZ 85719

REPORT DATE: September 2017

TYPE OF REPORT: Annual

PREPARED FOR: U.S. Army Medical Research and Materiel Command
Fort Detrick, Maryland 21702-5012

DISTRIBUTION STATEMENT: Approved for Public Release;
Distribution Unlimited

The views, opinions and/or findings contained in this report are those of the author(s) and should not be construed as an official Department of the Army position, policy or decision unless so designated by other documentation.

REPORT DOCUMENTATION PAGE

Form Approved
OMB No. 0704-0188

Public reporting burden for this collection of information is estimated to average 1 hour per response, including the time for reviewing instructions, searching existing data sources, gathering and maintaining the data needed, and completing and reviewing this collection of information. Send comments regarding this burden estimate or any other aspect of this collection of information, including suggestions for reducing this burden to Department of Defense, Washington Headquarters Services, Directorate for Information Operations and Reports (0704-0188), 1215 Jefferson Davis Highway, Suite 1204, Arlington, VA 22202-4302. Respondents should be aware that notwithstanding any other provision of law, no person shall be subject to any penalty for failing to comply with a collection of information if it does not display a currently valid OMB control number. **PLEASE DO NOT RETURN YOUR FORM TO THE ABOVE ADDRESS.**

1. REPORT DATE
September 2017

2. REPORT TYPE
Annual

3. DATES COVERED
1 Sep 2016 - 31 Aug 2017

4. TITLE AND SUBTITLE
Targeting the CRMP2-Ca2+ Channel Complex for Abortive Treatment of Migraine and Post-Traumatic Headache

5a. CONTRACT NUMBER

5b. GRANT NUMBER
W81XWH-16-1-0533

5c. PROGRAM ELEMENT NUMBER

5d. PROJECT NUMBER

5e. TASK NUMBER

5f. WORK UNIT NUMBER

6. AUTHOR(S)
Rajesh Khanna, Frank Porreca, Jennifer Yanhua Xie, Aubin Moutal, Nathan Eyde

E-Mail: frankp@email.arizona.edu

7. PERFORMING ORGANIZATION NAME(S) AND ADDRESS(ES)
University of Arizona,
1501 N. Campbell Ave.
Department of Pharmacology,
LSN 562,
Tucson, AZ 85724

8. PERFORMING ORGANIZATION REPORT

9. SPONSORING / MONITORING AGENCY NAME(S) AND ADDRESS(ES)

U.S. Army Medical Research and Materiel Command
Fort Detrick, Maryland 21702-5012

10. SPONSOR/MONITOR'S ACRONYM(S)

11. SPONSOR/MONITOR'S REPORT NUMBER(S)

12. DISTRIBUTION / AVAILABILITY STATEMENT

Approved for Public Release; Distribution Unlimited

13. SUPPLEMENTARY NOTES

14. ABSTRACT

Migraine is one of the world's most common neurological disorders. Current acute migraine treatments have sub-optimal efficacy and new therapeutic options are needed. Approaches targeting calcitonin gene related peptide (CGRP) signaling are clinically effective but small molecule antagonists have not been advanced due to toxicity. In this study, we explored the axonal growth/specification collapsin response mediator protein 2 (CRMP2) as a novel "druggable" target for inhibiting CGRP release and for potential relevance for treatment of migraine pain and post-traumatic headache. CRMP2 has been demonstrated to regulate N-type voltage gated Ca^{2+} channel (CaV2.2) activity and Ca^{2+}-dependent CGRP release in sensory neurons. The co-expression of CRMP2 with CaV2.2 and CGRP in trigeminal ganglia (TG) sensory neurons suggested the possibility of a novel approach to regulate CGRP release in the trigeminal system. Screening protocols surprisingly revealed that (S)-Lacosamide ((S)-LCM), an inactive analog of the clinically-approved small molecule anti-epileptic drug (R)-Lacosamide (Vimpat®), inhibited CRMP2 phosphorylation by cyclin dependent kinase 5 (Cdk5) in rat TG slices and decreased depolarization-evoked Ca^{2+} influx in TG cells in culture. (S)-LCM significantly blocked capsaicin-evoked CGRP release from dural nerve terminals in the rat ex vivo cranial cup preparation. Additionally, cephalic and extracephalic cutaneous allodynia (CA) induced in rats by activation of dural nociceptors with a cocktail of inflammatory mediators (IM), was inhibited by oral administration of (S)-LCM given at 30 min post-IM application. S-LCM also blocked the development of cephalic and extracephalic allodynia induced by nitric oxide (NO) donor given at 30 min prior to the NO donor injections in sumatriptan-induced latent sensitization model in rats.

15. SUBJECT TERMS

S-Lacosamide, migraine, CRMP2, Cav2.2, allodynia, capsaicin-evoked CGRP release, cranial cup, inflammatory mediators, nitric oxide donor, sodium channels, calcium channels,

16. SECURITY CLASSIFICATION OF:			17. LIMITATION OF ABSTRACT	18. NUMBER OF PAGES	19a. NAME OF RESPONSIBLE PERSON USAMRMC
a. REPORT	b. ABSTRACT	c. THIS PAGE			19b. TELEPHONE NUMBER *(include area code)*
Unclassified	Unclassified	Unclassified	Unclassified	27	

Table of Contents

Page

Introduction…….……..…..5

Body……..……..5

Key Research Accomplishments…….…….. 5

Conclusion……23

Reportable Outcomes…… 25

References……27

Appendices……27

1. **INTRODUCTION:**

Soldiers have a three-fold higher incidence of migraine than civilians. Post-traumatic headache (PTH) can occur following a traumatic brain injury (TBI) though the underlying mechanisms that are not understood. PTH often presents with a migraine phenotype and affects upwards of 97% of all soldiers with TBI. Current treatments are often inadequate. New treatments are urgently needed for migraine and PTH. CGRP has been linked to the migraine pathophysiology. The release of CGRP from either the peripheral or central processes of neurons depends on activation of Ca^{2+} channels including the CaV2.2 (N-type) channel, which is critically modulated by collapsin response mediator protein 2 (CRMP2). We have recently found that (*S*)-lacosamide ((*S*)-LCM), an *enantiomer* of the clinically approved anti-epileptic drug (*R*)-LCM, or Vimpat®, has preferential activity on Ca^{2+} channels through the modulation of CRMP2 phosphorylation. The goal of this application is to determine if (S)-LCM is effective in preclinical models of migraine by inhibiting interactions of CRMP2 and N-type calcium channels providing a rationale for advancement to human trials for migraine and for PTH.

2. **KEYWORDS:**

S-Lacosamide, migraine, CRMP2, Cav2.2, alloydnia, CGRP release, cranial cup, nitric oxide donor, voltage-gated sodium channels, voltage-gated calcium channels, excitability, constellation pharmacology

3. **ACCOMPLISHMENTS:**
   - **What were the major goals of the project?**

In this application, we propose to test the hypothesis that the small molecule (S)-lacosamide, ((S)-LCM), inhibits voltage-gated calcium channel CaV2.2 activity and calcitonin gene related peptide (CGRP) release providing a strong rationale for treatment of abortive migraine and post-traumatic headache (PTH). Migraine and PTH are a frequent complaint of soldiers. Decreasing CGRP activity has been clinically validated for migraine therapy. We have previously demonstrated that the axonal growth/specification collapsin response mediator protein 2 (CRMP2) regulates CaV2.2 activity and Ca^{2+}-dependent CGRP release in sensory neurons. CRMP2 levels are increased in chronic migraine patients. Our recent work demonstrates that (S)-LCM inhibits CRMP2 phosphorylation, inhibiting CaV2.2-CRMP2 association and CaV2.2 activity. (S)-LCM is the enantiomer of the clinically approved anti-epileptic drug Vimpat®. While (S)-LCM has not yet undergone clinical evaluation, it has drug-like qualities that likely allow rapid advancement to humans. (S)-LCM will be tested in vitro for functional activity in blocking Ca^{2+} currents in cultured trigeminal ganglion (TG) neurons identified to innervate the dura mater from rats. The efficacy, and duration of action, of (S)-LCM will be tested in two rodent models of migraine-related pain – dural inflammatory mediator (IM)-induced cutaneous allodynia (CA) and expression of nitric oxide donor-induced CA in animals with sumatriptan-induced latent sensitization (a model of migraine chronification and medication overuse headache, MOH). The ability of (S)-LCM to decrease CGRP levels in the jugular blood, a translational biomarker for migraine, will be assessed in the MOH model. We will also characterize the presence of CA in a model of repetitive mild traumatic brain injury (mTBI) and evaluate the possible efficacy of (S)-LCM in this model. We will employ constellation pharmacology to perform a phenotypic screening of TG neurons innervating the dura mater to develop molecular fingerprints of dural TG cells in migraine and PTH models as well as to identify the classes of neurons targeted by (S)-LCM. Finally, we will perform a comprehensive evaluation of the neurobehavioral toxicity of (S)-LCM to determine its therapeutic index for effects in dural trigeminal afferents in rats. These studies will justify rapid evaluation of (S)-LCM in subsequent IND-enablement studies and future clinical trials representing an entirely new

mechanism for abortive treatment of migraine and, possibly, PTH in soldiers and civilians.

The following aims has been proposed to be completed at the Khanna and Porreca Laboratories during the entire funding period:

- **Aim 1 (KHANNA lab)**. Efficacy and mechanism of (*S*)-LCM in blocking Ca^{2+} currents in cultured TG neurons innervating dura from rats. In this Aim, we will confirm the mechanism of action of (S)-LCM by investigating ionic changes in TGs from vehicle or sumatriptan-treated rats and on TGs from mice subjected to sham injury or to repetitive mild TBI in order to explore changes that may be relevant to "migrainous" biology.
    - **Aim 1.1**. Assessing inhibition of Cdk5-mediated phosphorylation of CRMP2 in TGs that innervate the dura mater.
    - **Aim 1.2**. Assess the inhibition of CRMP2-CaV2.2 association in these TG cells.
    - **Aim 1.3**. Test the inhibition of Ca^{2+} currents by (S)-LCM in cultured identified dural TG neurons.
    - **Aim 1.4**. Test the effects of (S)-LCM on excitability of TG neurons.
    - **Aim 1.5**. Perform a phenotypic screening of TG neurons innervating the dura mater utilizing the "constellation pharmacology" paradigm
- **Aim 2 (PORRECA Lab)**. Determine if (S)-LCM prevents periorbital and hindpaw cutaneous allodynia (CA) and blood CGRP elevation in rats. In this aim, the in vivo efficacy of (S)-LCM in inhibiting CA and CGRP plasma levels will be evaluated in 2 cephalic pain models using two different routes at multiple time points in male and female rats.
    - **Aim 2.1**. Does (S)-LCM abolish the development of CA induced by IM in rats?
    - **Aim 2.2**. Determine if (S)-LCM prevents nitric oxide (NO) donor-induced CA and blood CGRP elevation in rats with triptan-induced latent sensitization.
- **Aim 3 (PORRECA Lab).** Efficacy of (S)-LCM in cephalic pain from repetitive mild traumatic brain injury (rmTBI) in mice.
    - In **Aim 3.1** Assess the efficacy of S-LCM in abolishing TBI-induced allodynia in mice.
    - **Aim 3.2** will assess the possible presence of ongoing headache in mice with rmTBI. Establish CPP with iv ketorolac in TBI mice and then test the effect of S-LCM on blocking ketorolac-induced CPP.
    - **Aim 3.3** will determine the consequences of rmTBI on the function of nerves innervating the dura mater using the cranial cup preparation. Detect the release of CGRP by dural afferents in TBI mice and determine the effect of S-LCM.

- **Aim 4 (KHANNA lab).** Does (*S*)-LCM have significant adverse effects at therapeutic doses for treatment of cephalic pain and PTH?
    - In **Aim 4**, we will assess the potential liabilities of (S)-LCM preclinically as a step in advancement to humans using a battery of widely accepted rodent models.

- **What was accomplished under these goals?**
    1) Major activities: During this initial funding period, we have carried out some of the experiments proposed for all four Aims and obtained very promising results.
    2) Objectives: Our objectives during this period were to determine the efficacy of (S)-LCM in migraine models and to establish and characterize the mTBI model and stress-related PTH.
    3) Significant results: We have analyzed the changes in ionic conductances in the mouse model of post-traumatic headache (PTH) induced by mild

traumatic brain injury (mTBI) at early (Day1; D1) and late (D14 and 21) time points. We have tested two different oral doses of S-LCM (10 and 30 mg/kg) in two different migraine models in rats. We have also successfully characterized the mouse model of PTH induced by mTBI at early and late time points with or without stress.

Methods for **Aim 1**:

DRG isolation and culturing: Sensory DRG neurons from male C57BL/6J mice were isolated as described previously. Dorsal root ganglia (from thoracic 2 to lumbar 6 spinal levels) were excised aseptically and placed in Hank buffered salt solution (HBSS, Life technologies) containing penicillin (100 U/mL) and streptomycin (100 μg/mL, Cat# 15140, Life technologies) on ice. The ganglia were dissociated enzymatically by a 45 min incubation (37°C) in a DMEM (Cat# 11965, Life technologies) solution containing neutral protease (3.125 mg.ml-1, Cat#LS02104, Worthington) and collagenase Type I (5 mg.ml-1, Cat# LS004194, Worthington). The dissociated cells were resuspended in complete DRG medium, DMEM containing penicillin (100 U/mL), streptomycin (100 μg/mL), 30 ng.ml-1 nerve growth factor and 10% fetal bovine serum (Hyclone). For Ca2+ imaging, the cells were seeded on poly-D-lysine (Cat# P6407, Sigma) coated glass coverslips (Cat# 72196-15, electron microscopy sciences) as a drop of 20 μl on the center of each coverslip, then placed in a 37°C, 5 % CO2 incubator for 45–60 min to allow cells to attach. Then the cultures were flooded by gently adding complete DRG medium on the edge of each well to avoid detaching any weakly adherent cell. All cells were used within 24 to 48 hours after seeding.

Calcium imaging: DRG neurons were loaded at 37°C with 3μM Fura-2AM (Cat#F-1221, Life technologies, stock solution prepared at 1mM in DMSO, 0.02% pluronic acid, Cat#P-3000MP, Life technologies) for 30 minutes (K_d= 25μM, λ_{ex} 340, 380 nm/λ_{emi} 512 nm) to follow changes in intracellular calcium ($[Ca^{2+}]_c$) in Tyrode's solution (at ~310 mOsm) containing 119 mM NaCl, 2.5mM KCl, 2mM $MgCl_2$, 2mM $CaCl_2$, 25mM HEPES, pH 7.4 and 30mM glucose. The solution was supplemented with 500nM tetrodotoxin (TTX, voltage-gated Na^+ channel inhibitor) and 1 μM nifedipine (L-type voltage-gated Ca^{2+} channel inhibitor). Incubation with either (*R*)-LCM (200 μM) or (*S*)-LCM (200 μM, 20 μM, 2 μM, 200 nM, 20 nM, or 2 nM) was done during the loading of the cells with Fura-2AM and the drugs were also added to the excitatory solution. All calcium-imaging experiments were done at room temperature (~23°C), except those involving bath applications of innocuous (17°C) or cold (4°C) temperature stimuli. To isolate the contributions of particular channel subtypes, we used the following subunit-selective blockers (all purchased from Alomone Labs, Jerusalem): Nifedipine (10 μM, L-type); ω-agatoxin GIVA (200 nM, P/Q-type) [5]; ω-conotoxin-GVIA (500 nM, N-type) [3]; SNX-482 (200 nM, R-type) [6]; and 3,5-dichloro-N-[1-(2,2-dimethyl-tetrahydro-pyran-4-ylmethyl)-4-fluoro-piperidin-4-ylmethyl]-benzamide (TTA-P2, 1 μM, T-type) [2]. Baseline was acquired for 1 minute followed by stimulation (15 sec) with an excitatory solution (at ~310 mOsm) comprised of 32mM NaCl, 90mM KCl, 2mM $MgCl_2$, 2mM $CaCl_2$, 25mM HEPES, pH 7.4 and 30mM glucose. Fluorescence imaging was performed with an inverted microscope, Nikon Eclipse T*i*-U (Nikon Instruments Inc.), using objective Nikon Super Fluor MTB FLUOR 10x 0.50 and a Photometrics cooled CCD camera CoolSNAP ES^2 (Roper Scientific) controlled by NIS Elements software (version 4.20, Nikon instruments). The excitation light was delivered by a Lambda-LS system (Sutter Instruments). The excitation filters (340±5 nm and 380±7 nm) were controlled by a Lambda 10-2 optical filter change (Sutter Instruments). Fluorescence was recorded through a 505 nm dichroic mirror at 535±25 nm. To minimize photobleaching

and phototoxicity, the images were taken every 10 seconds during the time-course of the experiment using the minimal exposure time that provided acceptable image quality. The changes in $[Ca^{2+}]_c$ were monitored by following the ratio of F_{340}/F_{380}, calculated after subtracting the background from both channels.

Whole-cell voltage-clamp electrophysiology: Recordings were obtained from acutely dissociated DRG neurons as described. To isolate calcium currents, Na^+ and K^+ currents were blocked with 500 nM tetrodotoxin (TTX; Alomone Laboratories) and 30 mM tetraethylammonium chloride (TEA-Cl; Sigma). Extracellular recording solution (at ~310 mOsm) consisted of the following (in mM): 110 *N*-methyl-D-glucamine (NMDG), 10 $BaCl_2$, 30 TEA-Cl, 10 HEPES, 10 glucose, pH at 7.4, 0.001 TTX, 0.01 nifedipine. The intracellular recording solution (at ~310 mOsm) consisted of the following (in mM): contained 150 CsCl2, 10 HEPES, 5 Mg-ATP, 5 BAPTA, pH at 7.4. Fire-polished recording pipettes, 2 to 5 MV resistances were used for all recordings. Whole-cell recordings were obtained with a HEKA EPC-10 USB (HEKA Instruments Inc.); data were acquired with a Patchmaster (HEKA) and analyzed with a Fitmaster (HEKA). Capacitive artifacts were fully compensated, and series resistance was compensated by ~70%. Recordings made from cells with greater than a 5 mV shift in series resistance compensation error were excluded from analysis. All experiments were performed at room temperature (~23°C).

Constellation pharmacology: DRG neurons were loaded at 37°C with 3μM Fura-2AM for 30 minutes in Tyrode's solution. After a 1 minute baseline measurement Ca^{2+} influx was stimulated by the addition of the following receptor agonists: 400 nM menthol, 50 μM histamine, 10 μM adenosine triphosphate (ATP), 200 μM allyl isothiocyanate (AITC), 1 mM acetylcholine (Ach), 100 nM capsaicin diluted in Tyrode's solution (without TTX or Nifedipine). At the end of the constellation pharmacology protocol, cell viability was assessed by depolarization-induced Ca^{2+} influx using and an excitatory KCl solution comprised of 32mM NaCl, 90mM KCl, 2mM $MgCl_2$, 2mM $CaCl_2$, 25mM HEPES, pH 7.4, 30mM glucose. After the 1-minute baseline measurement, each trigger was applied for 15-seconds in the order indicated above in 6-minute intervals. Following each trigger, bath solution was continuously perfused over the cells to wash off excess of the trigger. This process was automated using the software WinTask x64 (Version 5.1, WinTask) that controlled the perfusion of the standard bath solution and triggers through Valvelink 8.2 software (Automate Scientific). For the (*S*)-LCM condition, 10 μM (*S*)-LCM was added to the Tyrode's solution during the loading with Fura-2AM, as well as to each of the solutions containing a trigger. Fluorescence imaging was performed under the same conditions noted above for calcium imaging. A cell was defined as a 'responder' if its fluorescence ratio of 340nm/380nm was greater than 10% of the baseline value calculated using the average fluorescence in the 30 seconds preceding application of the trigger.

Results for **Aim 1**: We used a mouse model of mild TBI (mTBI)[1; 4] as described by Kane and colleagues. Two time points were analyzed for characterization of potential alterations in ion channel functions. This is important as ion channels' functions in sensory neurons control the delivery and duration of action potentials leading to neurotransmitter release and nociceptive signal transmission. Neurotransmitter release relies on the entry of Ca^{2+} ions into the sensory neuron. Thus, we first looked if voltage gated Ca^{2+} channel function was altered after TBI. Dorsal root ganglia (DRG) sensory neurons were isolated from mice either 1 day or 14 days after TBI and compared to sham. Using electrophysiology, we measured the Ca^{2+} current

evoked by incremental depolarizing pulses (Figure 1A). No difference was found in the voltage-current relationship for voltage gated Ca^{2+} channels (Figure 1B). There was also no difference in the peak current density evoked by a +10 mV current. (Figure 1C). These results show no change in Ca^{2+} current density after a TBI.

We next asked if voltage gated Na^+ channels were altered after TBI. These channels participate to the initiation and the upstoke of action potentials. Dorsal root ganglia (DRG) sensory neurons were isolated from mice either 1 day or 14 days after TBI and compared to sham. Using electrophysiology, we measured the Na^+ current evoked by incremental depolarizing pulses (Figure 2A). No difference was found in the voltage-current relationship for voltage gated Na^+ channels (Figure 2B). There was also no significant difference in the peak current density evoked by a -20 mV current (Figure 2C). To note here, we observed a trend towards decreased Na^+ peak current density at -20 mV 1 day after TBI compared to sham ($p=0.1683$). These results show no change in Na^+ current density after a TBI.

Finally, we analyzed the function of A-type voltage gated K^+ channels. These channels participate to the recovery of the action potential and dysregulation of these channels will alter the duration of an action potential and the frequency of firing for the sensory neurons. Dorsal root ganglia (DRG) sensory neurons were isolated from mice either 1 day or 14 days after TBI and compared to sham. Using electrophysiology, we measured the K^+ current evoked by incremental depolarizing pulses (Figure 2A). No difference was found in the voltage-current relationship for voltage gated K^+ channels (Figure 3B). We also tested activation (Figure 3C) and inactivation (Figure 3D) properties for voltage gated K^+ channels. No difference was found for activation of the voltage gated K^+ channels (Figure 3C). We found a significant decrease of the inactivation of the voltage gated K^+ channels 14 days after TBI (Figure 3D). This indicates a delayed inactivation of the A-type voltage gated K^+ channels in sensory neurons 14 days after TBI. This event could lead to the delivery of prolonged action potentials.

We asked if voltage gated Na^+ channels could be altered in trigeminal ganglia neurons after TBI. Trigeminal ganglia (TG) sensory neurons were isolated from mice 1 day after TBI and compared to sham. Using electrophysiology, we measured the Na^+ current evoked by incremental depolarizing pulses (Figure 4A). No difference was found in the voltage-current relationship for voltage gated Na^+ channels (Figure 4B). There was also no significant difference in the peak current density evoked by a -20 mV current (Figure 4C). These results show no change in Na^+ current density in TG neurons 1 day after a TBI.

We used the recently described phenotypic screening method termed constellation pharmacology, which uses subtype-selective pharmacological agents to elucidate cell-specific combinations (constellations) of key signaling proteins that define specific cell types. The constellation pharmacology protocol consists of sequential challenges, applied 6-min apart, to test activity of Ca^{2+} permeable ligand-gated ion channels, metabotropic receptors and voltage-gated Ca^{2+} channels. At the end of each experiment, a membrane-depolarizing agent (i.e. KCl) is used to ensure neuronal viability; neurons that did not respond to this trigger were not analyzed. In each case the readout is a change in Ca^{2+} fluorescence. We applied the constellation pharmacology protocol to DRG neurons isolated from mice either 1 day or 14 days after TBI and compared to sham. Data from 3 independent experiments were collected and the responses of each neuron to each constellation pharmacology trigger were analyzed. Only DRGs with responses >10% over the baseline

fluorescence were considered in our analyses. We first asked if the sensitivity of DRG sensory neurons to the different agonist challenges could be altered 1 day or 14 days after TBI. We analyzed the percent of cells responding to a defined trigger, independently of any other trigger the cells may have responded to. In DRGs isolated from day 1 after TBI mice, we found an increased competence for ATP and a decreased competence for menthol. This suggests a gain of function of P2X receptors and a loss of function of TRPM8 channels 1 day after TBI. In DRGs isolated from day 14 after TBI mice, we found an increased number of neurons responding to the receptor agonist challenges (acetylcholine, AITC, ATP, histamine, menthol and capsaicin). This suggests a global sensitization of the DRG neurons 14 days after TBI. More precisely, AchR, TRPA1, P2X, H3R, TRPM8 and TRPV1 function is increased. We next asked if the overall competence of the neurons could be altered 1 day or 14 days after TBI by assessing if the DRGs responded to the same number of agonist challenges, independently of which compound they responded to (Figure. 5B). No difference was found on day 1 after TBI but DRG neurons showed increased functional competence on day 14 after TBI (Figure. 5B). This is illustrated by an increased number of DRG neurons responding to 2 – 5 receptor agonist challenges while less neurons were responding to only depolarization (90mM KCl) (Figure. 5B).

The above analyses do not take into account the extent of Ca^{2+} influx following each challenge. Therefore, here we analyzed peak Ca^{2+} responses of responders to the various triggers. We did not find any significant differences in DRGs isolated for day 1 after TBI mice. DRGs isolated from day 14 TBI mice showed a decreased response to histamine, menthol and capsaicin. We finally investigated the average peak Ca^{2+} response to 90 mM KCl stimulation of neurons that responded to a trigger, independent of any other compounds they responded to. DRGs isolated for day 1 after TBI mice had an increased depolarization-evoked Ca^{2+} influx in AITC, histamine or menthol responding neurons. Overall, K^{+}-evoked Ca^{2+} influx was increased in DRGs isolated from day 1 TBI mice. We found a decreased depolarization evoked Ca2+ influx for neurons responding to acetylcholine, AITC, histamine, menthol or capsaicin but not for neurons responding to ATP in DRGs isolated from day 14 TBI mice. Overall, the K+-evoked Ca2+ influx was decreased in these neurons. These results show a sensitization of voltage gated Ca^{2+} channels in sensory neurons 1 day after TBI and a desensitization a day after TBI.

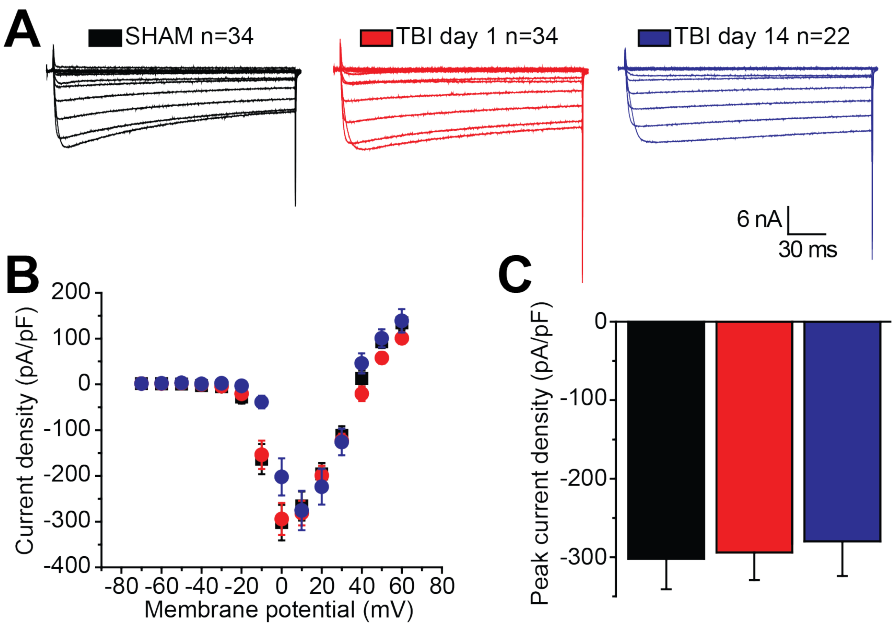

Figure 1. DRG sensory neurons Ca^{2+} currents are not altered after TBI. (**A**) Representative family of Ca^{2+} current traces are illustrated from sensory neurons isolated from Sham animals, 1 day after TBI (TBI day 1) or 14 days after TBI (TBI day 14). Currents were evoked by 200 ms prepulses between -90 mV to +60 mV, in 10 mV increments. (**B**) Summary of the total Ca^{2+} current versus voltage relationship (in pA/pF) from sensory neurons isolated from Sham animals, 1 day after TBI (TBI day 1) or 14 days after TBI (TBI day 14). (**C**) Peak current density, at +10 mV, for the indicated conditions. n=22-34 cells per condition (*$p<0.05$, one-way analysis of variance with Tukey's post hoc analysis). No difference was recorded between Sham animals and after 1 day or 14 days after TBI.

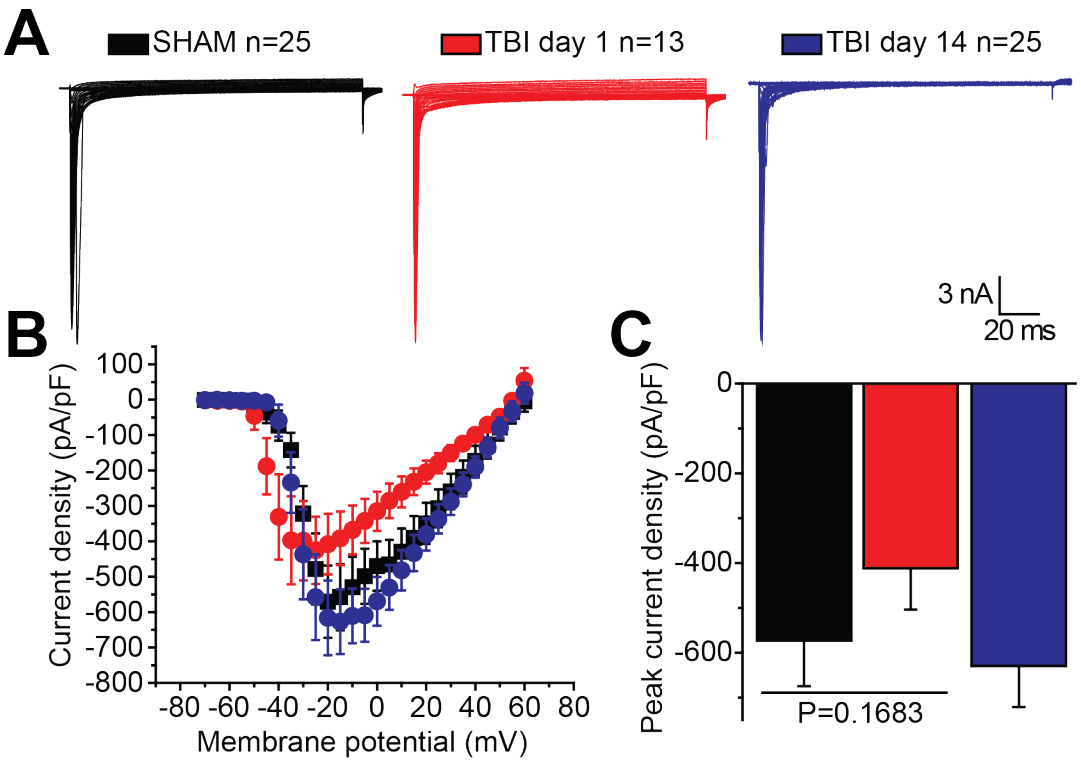

Figure 2. DRG sensory neurons Na^+ currents are not altered after TBI (**A**) Representative family of Na^+ current traces are illustrated from sensory neurons isolated from Sham animals, 1 day after TBI (TBI day 1) or 14 days after TBI (TBI day 14). Currents were evoked by 150 ms voltage steps from -70 mV to 60 mV in 5 mV increments. (**B**) Summary of the total Na^+ current versus voltage relationship (in pA/pF) from sensory neurons isolated from Sham animals, 1 day after TBI (TBI day 1) or 14 days after TBI (TBI day 14). (**C**) Peak current density, at -20 mV, for the indicated conditions. n=13-25 cells per condition (*$p<0.05$, one-way analysis of variance with Tukey's post hoc analysis). No difference was recorded between Sham animals and either 1 day or 14 days after TBI.

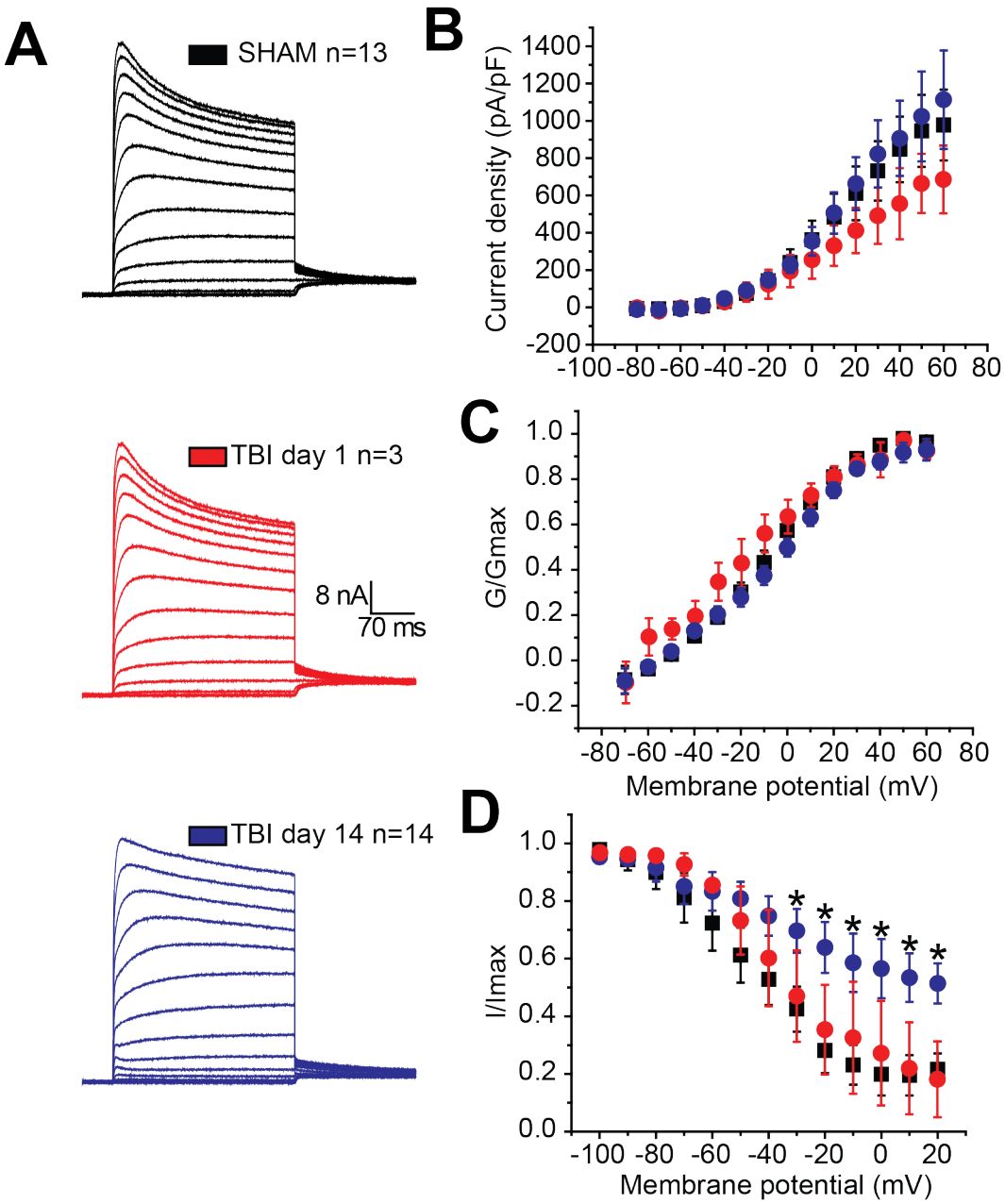

Figure 3. DRG sensory neurons K^+ currents are not altered after TBI (**A**) Representative family of I_KA (A-type K^+) current traces are illustrated from sensory neurons isolated from Sham animals, 1 day after TBI (TBI day 1) or 14 days after TBI (TBI day 14). The peak (**B**) I_KA in sensory neurons isolated from Sham animals, 1 day after TBI (TBI day 1) or 14 days after TBI (TBI day 14) are not different. The conductance–voltage relations for the peak (**C**). The points in (**C**) have been fitted by the Boltzmann relation and are shown as the continuous lines. (**D**) The steady-state inactivation of I_KA in neurons from. The steady-state inactivation voltage protocol consisted of a step to +60mV after prepulses to -100 mV. Currents were normalized to the maximal value of G obtained for the -100 mV prepulse. The data points have been fitted by the Boltzmann relation and are shown as a continuous line. At day 14 after TBI, I_KA currents showed less inactivation compared to Sham controls. Activation was determined by voltage steps 300 ms in duration, in 10 mV increments from -80 to 60 mV. Inactivation was measured by applying a 4 s conditioning prepulse (-100 to 20 mV in 20 mV increments) after which the voltage was stepped to 60 mV for 200 ms. n=3-14 cells per condition (*$p<0.05$, one-way analysis of variance with Tukey's post hoc analysis).

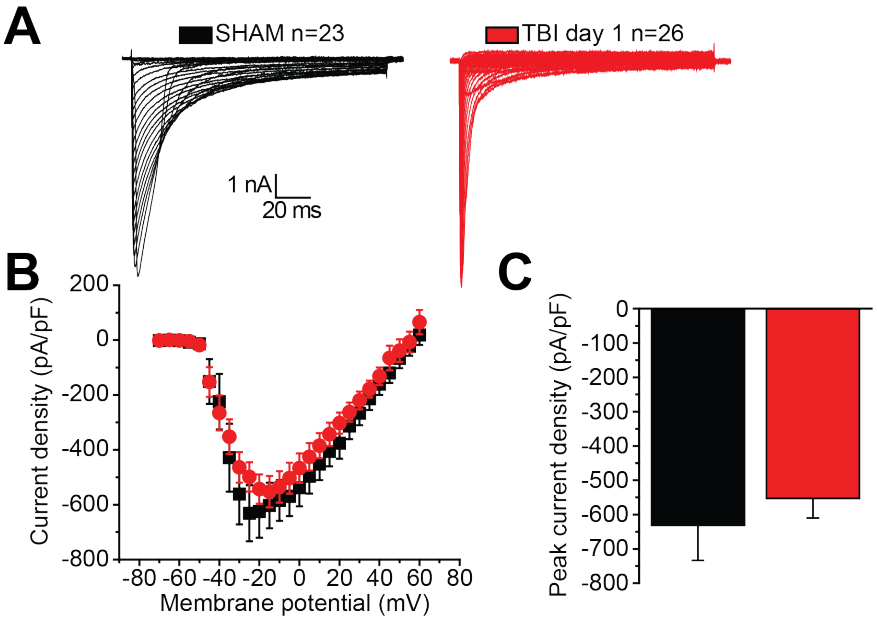

Figure 4. TG sensory neurons Na^+ currents are not altered after TBI. (**A**) Representative family of Na^+ current traces are illustrated from sensory neurons isolated from Sham animals and 1 day after TBI (TBI day 1). Currents were evoked by 150 ms voltage steps from -70 mV to 60 mV in 5 mV increments. (**B**) Summary of the total Na^+ current versus voltage relationship (in pA/pF) from sensory neurons isolated from Sham animals and 1 day after TBI (TBI day 1). (**C**) Peak current density, at -20 mV, for the indicated conditions. n=25-28 cells per condition (*$p<0.05$, one-way analysis of variance with Tukey's post hoc analysis). No difference was recorded between Sham animals and 1 day after TBI.

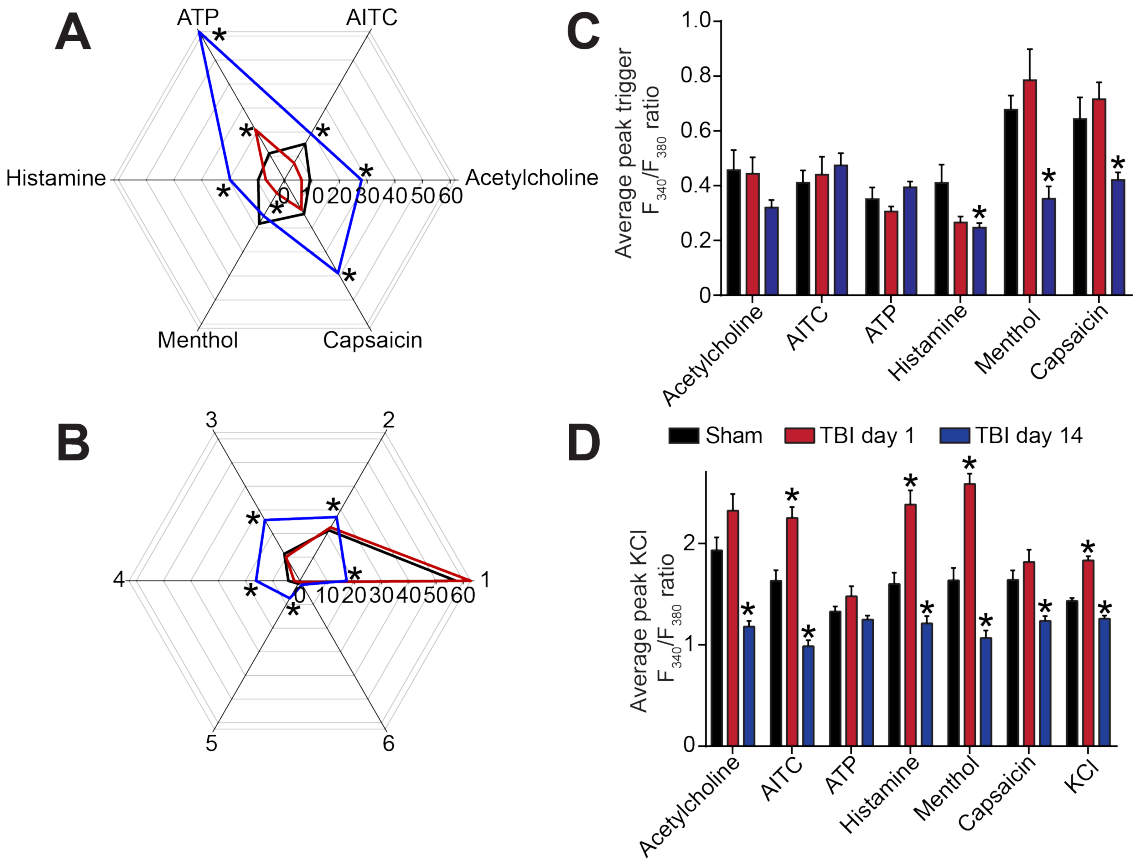

Figure 5. Functional 'fingerprinting' of DRG neuronal subclasses after TBI. In a typical experimental trial, the responses of >100 individual neurons were monitored simultaneously. Neurons were challenged using: menthol (400 nM), histamine (50 μM), ATP (10 μM), AITC (200 μM), acetylcholine (1 mM), capsaicin (100 nM) and KCl (90 mM). All cells were selected based on their response to the depolarizing pulse of KCl. (**A**) Polar plot showing the percent of cells responding to major classes of triggers. Data are from 4 independent experiments with a total n=1049 for control and n=571 for TBI day 1 and n= 541 for TBI day 14. (**B**) The response of DRG neurons to one or more constellation pharmacology trigger was analyzed. The polar plot indicates the percentage of cells that responded to the indicated number of triggers independently of which compound they responded to. The number 1 corresponds to the proportion of cells that responded to KCl only and no other trigger. Bar graphs showing the average peak response to the indicated trigger (**C**) or 90 mM KCl (**D**) in the major functional neuronal populations identified in panel **A**. (**H**) Bar graphs showing the average peak response to depolarization for cells showing a response to the indicated trigger independently of which other compound they responded to. (*, $p<0.05$; Student's t-test). AITC: allyl isothiocyanate, ATP: adenosine triphosphate, KCl: potassium chloride.

Methods and results for **Aim 2.1**: Sprague Dawley rats (Harlan) weighing 200–300 g were implanted with a guide cannula sitting on the dural surface without penetrating dura. After 7-10 days' recovery, the animals received injections of a cocktail of 10 µl inflammatory mediator (IM) or synthetic interstitial fluid (SIF, vehicle control) onto the dura. Behavioral responses to probing of the periorbital and hindpaw regions were obtained before and after dural injections using von Frey (VF) filaments by an investigator blinded to the treatments.

Dural IM produced robust cephalic and extracephalic pain. Low pH SIF also produced cutaneous allodynia. Oral administration of S-LCM dose-dependently abolished the development of periorbital and hindpaw allodynia when given at 30 min post-IM or low pH SIF (**Figure 6**).

Figure 6. Abolishment of IM-induced cephalic and extracephalic allodynia by S-LCM. A) Study Design. SD rats were baselined for periorbital and hindpaw tactile threshold and received an injection of IM (B, C) or SIF (D, E) onto the dural surface. S-LCM (10 or 30 mg/kg, p.o.) or vehicle (10% DMSO/90% DIH2O) were administered at 30 min post-IM/SIF. The periorbital (B, D) and hindpaw (C, E) tactile thresholds were measured hourly for 5 hours following IM or SIF injection. The red arrow illustrates the direction the direction of "more pain" in the graphs. Low dose of S-LCM (10 mg/kg, p.o.) did not alter cephalic allodynia (B), but partially abolished hindpaw (C) allodynia induced by IM, while 30 mg/kg, p.o. dose of S-LCM blocked both measures. Low pH alone also induced periorbital (D) and hindpaw (E) allodynia that was blocked by 30 mg/kg p.o. S-LCM. The area over the time-effect curve (AOC) of the periorbital (F) and hindpaw (G) allodynia also suggested the effective blockade of cephalic and extracephalic allodynia by 30 mg/kg S-LCM. Group sizes are shown on the bar graph. Two-way ANOVA *post hoc* Dunnett's multiple comparison test was used for B, C, D, E; One way ANOVA *post hoc* Tukey's multiple comparison test was used for F, G. Significant level was set at $p<0.05$.

Figure 6.

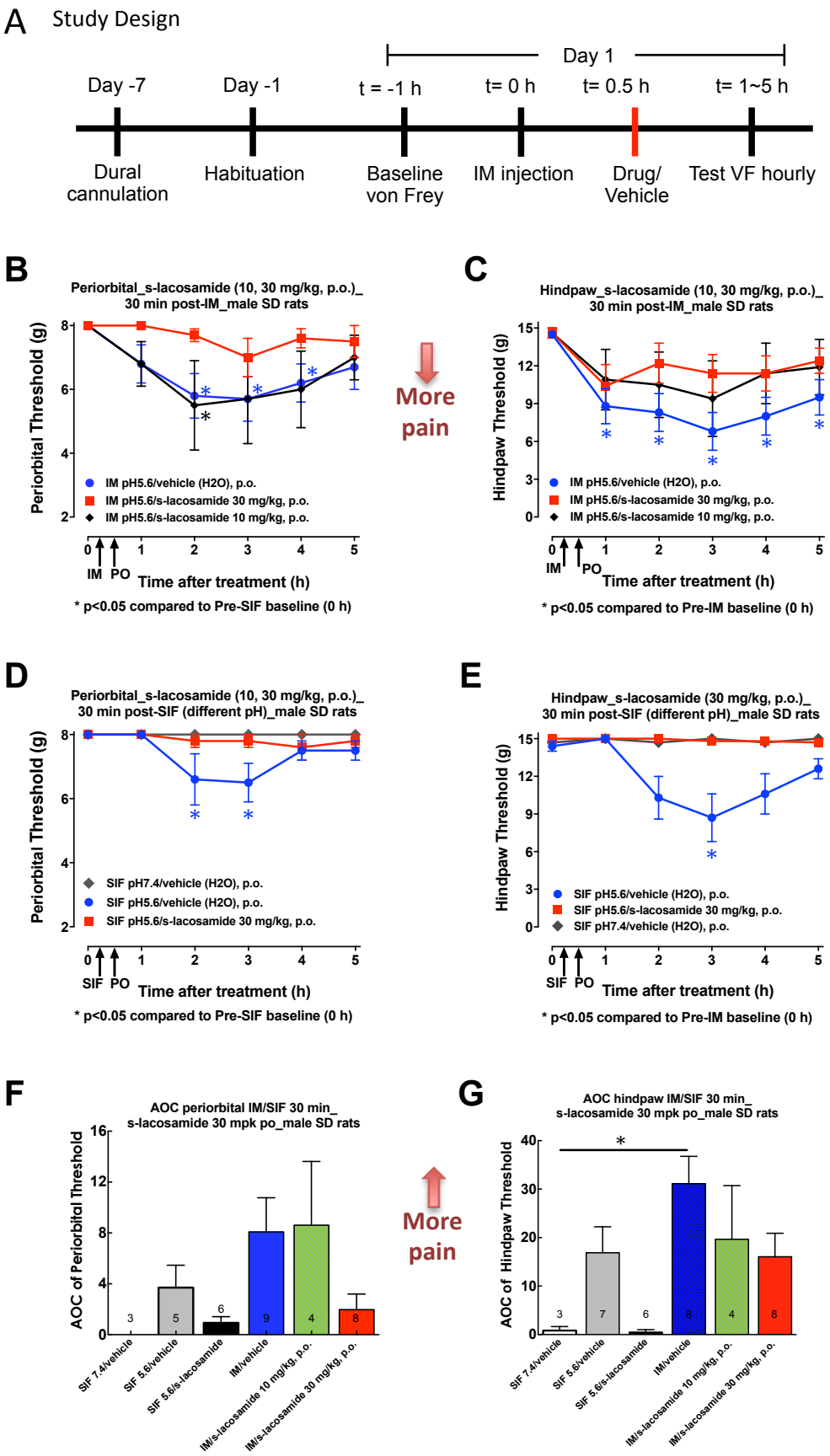
A
Study Design
Day 1
Day -7
Day -1
t = -1 h
t= 0 h
t= 0.5 h
t= 1~5 h
Dural cannulation
Habituation
Baseline von Frey
IM injection
Drug/ Vehicle
Test VF hourly
B
Periorbital_s-lacosamide (10, 30 mg/kg, p.o.)_ 30 min post-IM_male SD rats
Periorbital Threshold (g)
IM pH5.6/vehicle (H2O), p.o.
IM pH5.6/s-lacosamide 30 mg/kg, p.o.
IM pH5.6/s-lacosamide 10 mg/kg, p.o.
IM PO
Time after treatment (h)
* p<0.05 compared to Pre-SIF baseline (0 h)
More pain
C
Hindpaw_s-lacosamide (10, 30 mg/kg, p.o.)_ 30 min post-IM_male SD rats
Hindpaw Threshold (g)
IM pH5.6/vehicle (H2O), p.o.
IM pH5.6/s-lacosamide 30 mg/kg, p.o.
IM pH5.6/s-lacosamide 10 mg/kg, p.o.
IM PO
Time after treatment (h)
* p<0.05 compared to Pre-IM baseline (0 h)
D
Periorbital_s-lacosamide (10, 30 mg/kg, p.o.)_ 30 min post-SIF (different pH)_male SD rats
Periorbital Threshold (g)
SIF pH7.4/vehicle (H2O), p.o.
SIF pH5.6/vehicle (H2O), p.o.
SIF pH5.6/s-lacosamide 30 mg/kg, p.o.
SIF PO
Time after treatment (h)
* p<0.05 compared to Pre-SIF baseline (0 h)
E
Hindpaw_s-lacosamide (30 mg/kg, p.o.)_ 30 min post-SIF (different pH)_male SD rats
Hindpaw Threshold (g)
SIF pH5.6/vehicle (H2O), p.o.
SIF pH5.6/s-lacosamide 30 mg/kg, p.o.
SIF pH7.4/vehicle (H2O), p.o.
SIF PO
Time after treatment (h)
* p<0.05 compared to Pre-IM baseline (0 h)
F
AOC periorbital IM/SIF 30 min_ s-lacosamide 30 mpk po_male SD rats
AOC of Periorbital Threshold
SIF 7.4/vehicle
SIF 5.6/vehicle
SIF 5.6/s-lacosamide
IM/vehicle
IM/s-lacosamide 10 mg/kg, p.o.
IM/s-lacosamide 30 mg/kg, p.o.
More pain
G
AOC hindpaw IM/SIF 30 min_ s-lacosamide 30 mpk po_male SD rats
AOC of Hindpaw Threshold
SIF 7.4/vehicle
SIF 5.6/vehicle
SIF 5.6/s-lacosamide
IM/vehicle
IM/s-lacosamide 10 mg/kg, p.o.
IM/s-lacosamide 30 mg/kg, p.o.

Methods and results for **Aim 2.2**: Female or male SD rats received s.c. infusions of sumatriptan (0.6 mg/kg/day, s.c.) or saline by implanted minipumps to establish "latent sensitization", followed by a 14 day drug-free period. Sodium nitroprusside (3 mg/kg, i.p.) was injected at D21 post the initial sumatriptan infusion. Periortibal and hindpaw allodynia was evaluated before and after SNP hourly for 5 hours following SNP injection. Only animals pretreated with sumatriptan infusion showed periorbital and hindpaw allodynia after NO-donor challenge[7]. (*S*)-LCM administered at 30 min prior to SNP blocked the development of both cephalic and extracephalic allodynia (**Figure 7**).

Figure 7. Blockade of nitric oxide (NO) donor-induced cephalic and extracephalic allodynia by S-LCM. A) Study Design. Female (B-E) and male (F-I) SD rats were baselined for periorbital and hindpaw tactile threshold and received an injection of S-LCM (30 mg/kg, p.o.) or vehicle (10% DMSO/90% DIH2O). 30 min later, sodium nitroprusside (SNP, 3 mg/kg, i.p.) were administered. The periorbital (B, F) and hindpaw (C, G) were measured hourly for 5 hours following SNP injection. The red arrow illustrates the direction of "more pain" in the graphs. Group sizes are marked on the graphs. S-LCM blocked both periorbital and hindpaw allodynia in both female and male rats. The area over the time-effect curve (AOC) of the periorbital (D, H) and hindpaw (E, I) allodynia also suggested the effective blockade of cephalic and extracephalic allodynia by 30 mg/kg S-LCM. Two-way ANOVA *post hoc* Dunnett's multiple comparison test was used for B, C, F, G; One way ANOVE *post hoc* Tukey's multiple comparison test was used for D, E; unpaired t-test was applied for H, I. Significant level was set at $p<0.05$.

Figure 7.

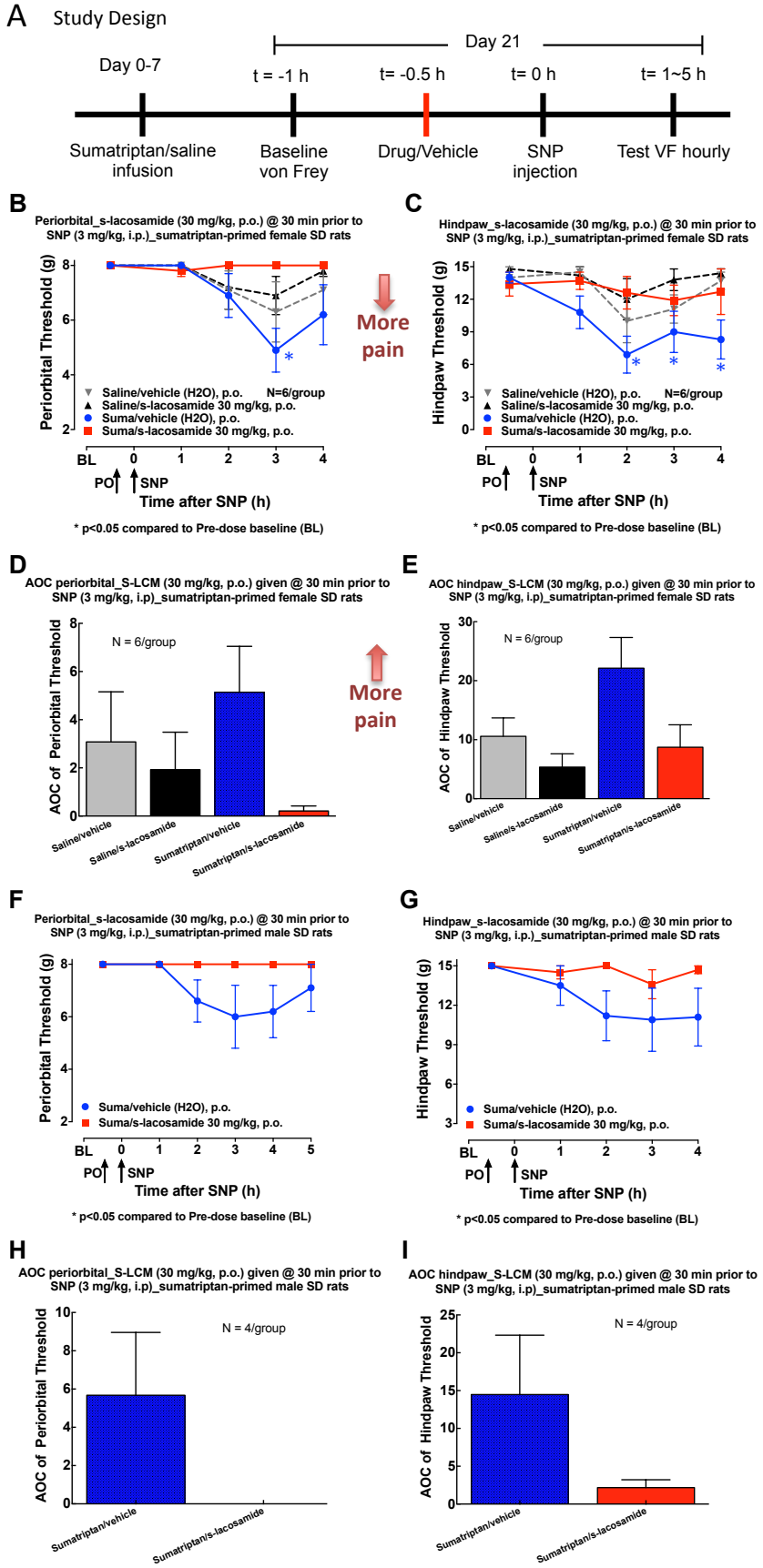
A
Study Design
Day 21
Day 0-7
t = -1 h
t= -0.5 h
t= 0 h
t= 1~5 h
Sumatriptan/saline infusion
Baseline von Frey
Drug/Vehicle
SNP injection
Test VF hourly
B
Periorbital_s-lacosamide (30 mg/kg, p.o.) @ 30 min prior to SNP (3 mg/kg, i.p.)_sumatriptan-primed female SD rats
Periorbital Threshold (g)
Saline/vehicle (H2O), p.o. N=6/group
Saline/s-lacosamide 30 mg/kg, p.o.
Suma/vehicle (H2O), p.o.
Suma/s-lacosamide 30 mg/kg, p.o.
BL
PO
SNP
Time after SNP (h)
* p<0.05 compared to Pre-dose baseline (BL)
More pain
C
Hindpaw_s-lacosamide (30 mg/kg, p.o.) @ 30 min prior to SNP (3 mg/kg, i.p.)_sumatriptan-primed female SD rats
Hindpaw Threshold (g)
Saline/vehicle (H2O), p.o. N=6/group
Saline/s-lacosamide 30 mg/kg, p.o.
Suma/vehicle (H2O), p.o.
Suma/s-lacosamide 30 mg/kg, p.o.
BL
PO
SNP
Time after SNP (h)
* p<0.05 compared to Pre-dose baseline (BL)
D
AOC periorbital_S-LCM (30 mg/kg, p.o.) given @ 30 min prior to SNP (3 mg/kg, i.p)_sumatriptan-primed female SD rats
AOC of Periorbital Threshold
N = 6/group
Saline/vehicle
Saline/s-lacosamide
Sumatriptan/vehicle
Sumatriptan/s-lacosamide
More pain
E
AOC hindpaw_S-LCM (30 mg/kg, p.o.) given @ 30 min prior to SNP (3 mg/kg, i.p)_sumatriptan-primed female SD rats
AOC of Hindpaw Threshold
N = 6/group
Saline/vehicle
Saline/s-lacosamide
Sumatriptan/vehicle
Sumatriptan/s-lacosamide
F
Periorbital_s-lacosamide (30 mg/kg, p.o.) @ 30 min prior to SNP (3 mg/kg, i.p.)_sumatriptan-primed male SD rats
Periorbital Threshold (g)
Suma/vehicle (H2O), p.o.
Suma/s-lacosamide 30 mg/kg, p.o.
BL
PO
SNP
Time after SNP (h)
* p<0.05 compared to Pre-dose baseline (BL)
G
Hindpaw_s-lacosamide (30 mg/kg, p.o.) @ 30 min prior to SNP (3 mg/kg, i.p.)_sumatriptan-primed male SD rats
Hindpaw Threshold (g)
Suma/vehicle (H2O), p.o.
Suma/s-lacosamide 30 mg/kg, p.o.
BL
PO
SNP
Time after SNP (h)
* p<0.05 compared to Pre-dose baseline (BL)
H
AOC periorbital_S-LCM (30 mg/kg, p.o.) given @ 30 min prior to SNP (3 mg/kg, i.p)_sumatriptan-primed male SD rats
AOC of Periorbital Threshold
N = 4/group
Sumatriptan/vehicle
Sumatriptan/s-lacosamide
I
AOC hindpaw_S-LCM (30 mg/kg, p.o.) given @ 30 min prior to SNP (3 mg/kg, i.p)_sumatriptan-primed male SD rats
AOC of Hindpaw Threshold
N = 4/group
Sumatriptan/vehicle
Sumatriptan/s-lacosamide

Methods and results for **Aim 3.1**: We used a mouse model of mild TBI (mTBI)[1; 4] as described by Kane and colleagues. Briefly, male C57BL/6J mice were acclimated to the von Frey chambers daily for 5 days of 3 h each. After baseline of periorbital and hindpaw tactile threshold, the animals received a 100 g weight dropped from 100 cm above the skull to the top of the head between bregma and lambda once. Mice spontaneously recovered the righting reflex and showed no evidence of seizures, paralysis or impaired behavior. Skull fracture and intracranial bleeding were not observed. The cutaneous allodynia was measured at various time points as the surrogate marker of PTH. The results showed that minor deficits in motor coordination and locomotor hyperactivity recovered over time. Significant elongation of the time for the animals to regain righting reflex was observed in mTBI compared to sham treated mice immediately after the trauma. Apparent periorbital and hindpaw allodynia was observed at 24 h after the mTBI, which slowly resolved by 14 days post-TBI. However, when the previously injured mice received bright light stress, the cephalic and extracephalic allodynia were precipitated again (**Figure 8**).

Figure 8. Time course of PTH induced by mTBI in mice. A) Study Design. Male C57BL/6J mice were baselined for periorbital and hindpaw tactile threshold after 5 days of acclimation. They then received a mild concussion by a 100 g metal bar dropped from 100 cm height under isoflurane anesthesia. Sham treated mice were only anesthetized with isoflurane. The righting time (B) and periorbital (C) and hindpaw (D) tactile threshold were measured at days 1, 4, 7 and 13 post-TBI. At D14, when the tactile threshold went back to normal, the animals were exposed to 30 min bright light stress (BLS, ~1000 Lux). And the periorbital (E) and hindpaw (F) tactile threshold were measured hourly at 1-5 h post-BLS. The red arrow illustrates the direction of "more pain" in the graphs. Group sizes are marked on the graphs. Unpaired t-test (B); Two-way ANOVA *post hoc* Dunnett's multiple comparison test (C, D); or One-way ANOVE *post hoc* Tukey's multiple comparison test (E, F) was used for statistical analysis. Significant level was set at $p<0.05$.

Figure 8.

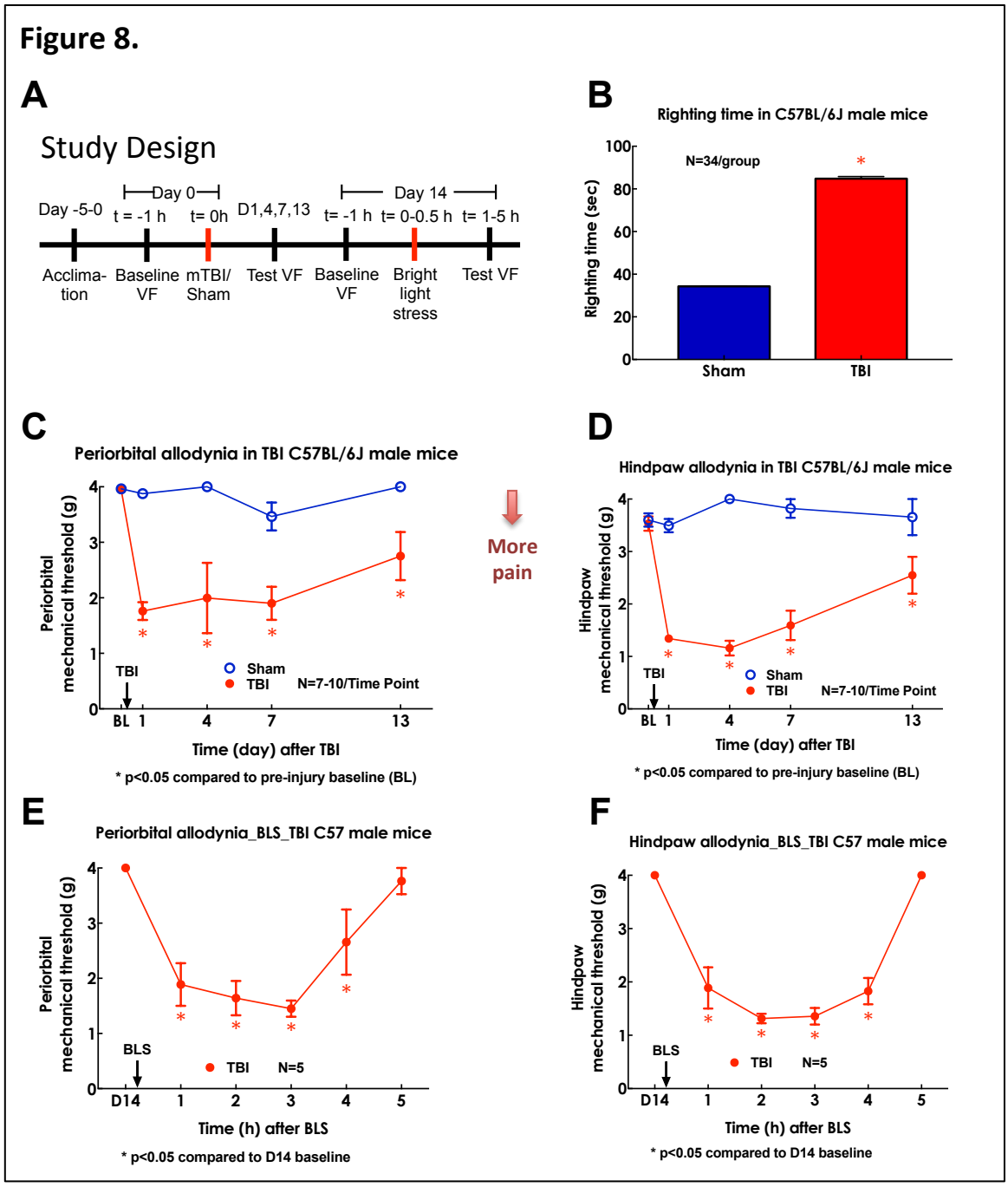
A
Study Design
Day -5-0
Day 0
t = -1 h
t= 0h
D1,4,7,13
Day 14
t= -1 h
t= 0-0.5 h
t= 1-5 h
Acclima-tion
Baseline VF
mTBI/ Sham
Test VF
Baseline VF
Bright light stress
Test VF
B
Righting time in C57BL/6J male mice
N=34/group
Righting time (sec)
Sham
TBI
C
Periorbital allodynia in TBI C57BL/6J male mice
Periorbital mechanical threshold (g)
TBI
Sham
TBI
N=7-10/Time Point
Time (day) after TBI
* p<0.05 compared to pre-injury baseline (BL)
More pain
D
Hindpaw allodynia in TBI C57BL/6J male mice
Hindpaw mechanical threshold (g)
TBI
Sham
TBI
N=7-10/Time Point
Time (day) after TBI
* p<0.05 compared to pre-injury baseline (BL)
E
Periorbital allodynia_BLS_TBI C57 male mice
Periorbital mechanical threshold (g)
BLS
TBI
N=5
Time (h) after BLS
* p<0.05 compared to D14 baseline
F
Hindpaw allodynia_BLS_TBI C57 male mice
Hindpaw mechanical threshold (g)
BLS
TBI
N=5
Time (h) after BLS
* p<0.05 compared to D14 baseline

Methods and results for **Aim 4**:

Rotarod: Following placement of the intrathecal catheters, the rats were trained to walk on a rotating rod (10 rev/min; Rotamex 4/8 device) with a maximal cutoff time of 180 seconds. Training was initiated by placing the rats on a rotating rod and allowing them to walk on the rotating rod until they either fell off or 180 seconds was reached. This process was repeated 6 times and the rats were allowed to recover for 24 hours before beginning the treatment session. Prior to treatment, the rats were run once on a moving rod in order to establish a baseline value. Saline or peptides were administered spinally via the intrathecal catheter. Assessment consisted of placing the rats on the moving rod and timing until either they fell off or reached a maximum of 180 seconds. This was repeated every 15 minutes for the first hour after drug administration and 30 minutes for the 4 hours after for a maximum time course of 5 hours.

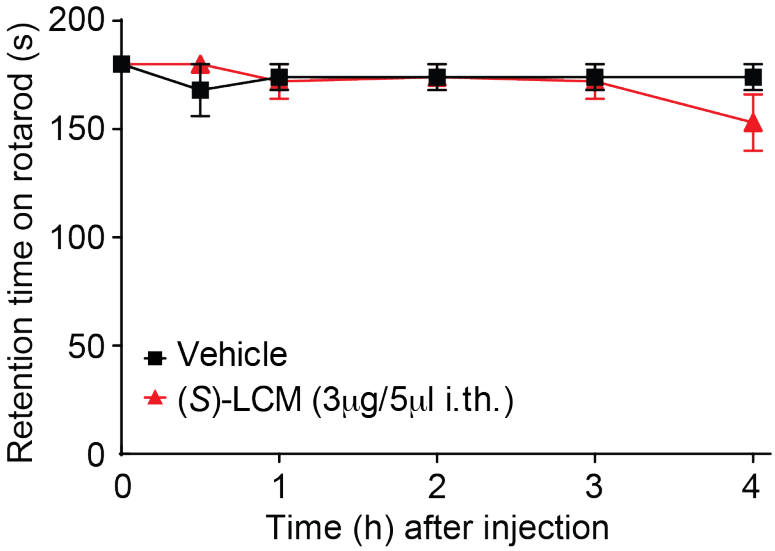

Figure 9. Spinal administration of (*S*)-LCM does not result in motor deficits or sedation. (*S*)-LCM (3 μg/5 μL i.th.) or vehicle (0.9 % saline) was evaluated for motor deficits using the rotarod performance test. Vehicle-treated animals and (*S*)-LCM –treated animals remained on the rotarod for 180 seconds at each time point over the course of 240 minutes. Animals treated with (*S*)-LCM remained on the rotarod for an average of 178 seconds, a value that was not significantly different from vehicle treated animals and baseline values. N=6 rats per condition.

Summary: This funding period has allowed us to meet many of our primary goals. We have not experienced technical problems and our experiments are progressing in a timely fashion.

- **What opportunities for training and professional development has the project provided?**

  Nothing to report.

- **How were the results disseminated to communities of interest?**

  Nothing to Report.

- **What do you plan to do during the next reporting period to accomplish the goals?**
  - The Khanna lab will continue on our goals for Aim 1.2 and begin Aim 4 in the next funding period.
  - The Porrreca lab will continue on our goals for Aims 2 and 3.1 in the next funding period.

4. **IMPACT:** *Describe distinctive contributions, major accomplishments, innovations, successes, or any change in practice or behavior that has come about as a result of the project relative to:*
   - **What was the impact on the development of the principal discipline(s) of the project?**
     - We have demonstrated the remarkable efficacy of S-LCM in mitigating cephalic and extracephalic allodynia in two different migraine models triggered by direct dural activation (IM model) or precipitated by bright light stress (MOH latent sensitization model) in rats given *as either abortive therapy or prophylactic therapy*. These results will greatly facilitate the rational for transition of S-LCM from the laboratory to human trials.
     - We have also characterized the mouse model of mild traumatic brain injury (mTBI)-induced cephalic and extracephalic allodynia as well as latent sensitization to bright light stress. One application of the mild TBI caused long-lasting sensitization of the animals to bright light stress even after the initial cephalic pain resolved. The ionic conductances are largely unchanged by the injury is an interesting and unexpected finding of this study thus far. These results set the foundation to test the efficacy of S-LCM to treat PTH in mice.

   - **What was the impact on other disciplines?**

     Nothing to Report.

   - **What was the impact on technology transfer?**

     Nothing to Report.

   - **What was the impact on society beyond science and technology?**

     Nothing to Report.

5. **CHANGES/PROBLEMS:**
   - **Changes in approach and reasons for change**
   - **Actual or anticipated problems or delays and actions or plans to resolve them**

- **Changes that had a significant impact on expenditures**
- **Significant changes in use or care of human subjects, vertebrate animals, biohazards, and/or select agents**
- **Significant changes in use or care of human subjects**
- **Significant changes in use or care of vertebrate animals.**
- **Significant changes in use of biohazards and/or select agents**

Nothing to Report

6. **PRODUCTS:** *List any products resulting from the project during the reporting period. If there is nothing to report under a particular item, state "Nothing to Report."*
   - **Publications, conference papers, and presentations**
     - **Journal publications.**
     - **Books or other non-periodical, one-time publications.**
     - **Other publications, conference papers, and presentations.**

       Nothing to report.

   - **Website(s) or other Internet site(s)**

     Nothing to report.

   - **Technologies or techniques**

     Nothing to report.

   - **Inventions, patent applications, and/or licenses**

     Nothing to report.

   - **Other Products**

     Nothing to report.

7. **PARTICIPANTS & OTHER COLLABORATING ORGANIZATIONS**
   - **What individuals have worked on the project?**

Name:	**Frank Porreca**
Project Role:	PI
Researcher Identifier (e.g. ORCID ID):	
Nearest person month worked:	2
Contribution to Project:	Dr. Porreca advised the whole team and provided oversight for the entire project.
Funding Support:	NA
Name:	**Yanhua Xie (Jennifer)**

Project Role:	Senior Scientist
Researcher Identifier (e.g. ORCID ID):	
Nearest person month worked:	6
Contribution to Project:	Dr. Xie designed the study, coordinated the work flow, provided blinding, analyzed the data and wrote the report.
Funding Support:	NA
Name:	**Nathan Eyde**
Project Role:	Research Technician
Researcher Identifier (e.g. ORCID ID):	
Nearest person month worked:	8
Contribution to Project:	Mr. Eyde executed the rat experiments, and collected the behavioral data.
Funding Support:	NA
Name:	**Chaoling Qu**
Project Role:	Research Scientist
Researcher Identifier (e.g. ORCID ID):	
Nearest person month worked:	8
Contribution to Project:	Ms. Qu executed the mouse experiments, and collected the behavioral data.
Funding Support:	NA
Name:	**Rajesh Khanna**
Project Role:	PI
Researcher Identifier (e.g. ORCID ID):	0000-0002-9066-2969
Nearest person month worked:	2
Contribution to Project:	Dr. Khanna advised the whole team and provided oversight for the entire project.
Funding Support:	NA
Name:	**Aubin Moutal**

Project Role:	Research Scientist
Researcher Identifier (e.g. ORCID ID):	
Nearest person month worked:	4
Contribution to Project:	Dr. Moutal executed the constellation pharmacology experiments
Funding Support:	NA
Name:	**Wennan Li**
Project Role:	Research Scientist
Researcher Identifier (e.g. ORCID ID):	
Nearest person month worked:	6
Contribution to Project:	Dr. Li executed the electrophysiology in both DRG and TG neurons.
Funding Support:	NA
Name:	**Song Cai**
Project Role:	Research Scientist
Researcher Identifier (e.g. ORCID ID):	
Nearest person month worked:	6
Contribution to Project:	Dr. Li executed the electrophysiology in both DRG and TG neurons.
Funding Support:	NA

- **Has there been a change in the active other support of the PD/PI(s) or senior/key personnel since the last reporting period?**
    - **Organization Name:**
    - **Location of Organization:**
    - **Partner's contribution to the project)**
        - **Financial support;**
        - **In-kind support**;
        - **Facilities**;
        - **Collaboration**;
        - **Personnel exchanges**
        - **Other.**

Nothing to Report.

8. **SPECIAL REPORTING REQUIREMENTS**
   - **COLLABORATIVE AWARDS:**

Two separate reports for Drs. Khanna and Porreca have been submitted to https://ers.amedd.army.mil for each award.

.

   - **QUAD CHARTS:**

NA

REFERENCES:

[1] Benromano T, Defrin R, Ahn AH, Zhao J, Pick CG, Levy D. Mild closed head injury promotes a selective trigeminal hypernociception: implications for the acute emergence of post-traumatic headache. Eur J Pain 2015;19(5):621-628.

[2] Choe W, Messinger RB, Leach E, Eckle VS, Obradovic A, Salajegheh R, Jevtovic-Todorovic V, Todorovic SM. TTA-P2 is a potent and selective blocker of T-type calcium channels in rat sensory neurons and a novel antinociceptive agent. MolPharmacol 2011;80(5):900-910.

[3] Feng ZP, Hamid J, Doering C, Bosey GM, Snutch TP, Zamponi GW. Residue Gly1326 of the N-type calcium channel alpha 1B subunit controls reversibility of omega-conotoxin GVIA and MVIIA block. The Journal of biological chemistry 2001;276(19):15728-15735.

[4] Kane MJ, Angoa-Perez M, Briggs DI, Viano DC, Kreipke CW, Kuhn DM. A mouse model of human repetitive mild traumatic brain injury. J Neurosci Methods 2012;203(1):41-49.

[5] Mintz IM, Venema VJ, Swiderek KM, Lee TD, Bean BP, Adams ME. P-type calcium channels blocked by the spider toxin omega-Aga-IVA. Nature 1992;355(6363):827-829.

[6] Newcomb R, Szoke B, Palma A, Wang G, Chen X, Hopkins W, Cong R, Miller J, Urge L, Tarczy-Hornoch K, Loo JA, Dooley DJ, Nadasdi L, Tsien RW, Lemos J, Miljanich G. Selective peptide antagonist of the class E calcium channel from the venom of the tarantula Hysterocrates gigas. Biochemistry 1998;37(44):15353-15362.

[7] Pradhan AA, Smith ML, McGuire B, Tarash I, Evans CJ, Charles A. Characterization of a novel model of chronic migraine. Pain 2014;155(2):269-274.

APPENDICES:

None.